



Universidad Autónoma
de Madrid

Biblos-e Archivo
Repositorio Institucional UAM

Repositorio Institucional de la Universidad Autónoma de Madrid
<https://repositorio.uam.es>

Esta es la **versión de autor** del artículo publicado en:
This is an **author produced version** of a paper published in:

BBA - Molecular Basis of Disease 1867. 12 (2021): 166241

DOI: <https://doi.org/10.1016/j.bbadis.2021.166241>

Copyright: © 2020. This manuscript version is made available under the CC-BY-NC-ND 4.0 licence <http://creativecommons.org/licenses/by-nc-nd/4.0/>

El acceso a la versión del editor puede requerir la suscripción del recurso
Access to the published version may require subscription

Resolvin-D1 prevents Angiotensin II-induced cardiac remodeling and hypertension by attenuation of cardiac inflammation

Francisco Olivares-Silva¹, Nicole De Gregorio², Jenaro Espitia-Corredor¹, Claudio Espinoza¹, Raúl Vivar³, José Miguel Osorio¹, Sergio Lavandero⁴, Concepción Peiró⁵, Carlos Sánchez-Ferrer⁵, Guillermo Díaz-Araya^{1,4}

Short title: RvD1 prevents hypertension by reducing inflammation

1 Department of Chemical Pharmacology and Toxicology, Faculty of Chemical Sciences and Pharmacy, University of Chile, Santiago, Chile

2 Mitchell Center for Alzheimer's Disease and Related Brain Disorders, Department of Neurology, University of Texas McGovern Medical School at Houston, Houston, TX, USA.

3 Pharmacology Program, Biomedical Sciences Institute, Faculty of Medicine, University of Chile, Santiago, Chile

4 Advanced Center for Chronic Diseases (ACCDiS), Faculty of Chemical Sciences and Pharmacy, and Faculty of Medicine, University of Chile, Santiago, Chile

5 Department of Pharmacology, Faculty of Medicine, Universidad Autónoma de Madrid and Instituto de Investigación Sanitaria Hospital Universitario La Paz (IdiPAZ), Spain

Category of the manuscript: original article

***Correspondence:** Guillermo Díaz-Araya, Department of Chemical Pharmacology and Toxicology and Advanced Center for Chronic Diseases (ACCDiS), Faculty of Chemical Sciences and Pharmacy, University of Chile; 8380492 Santiago, Chile. Tel: +562 29782975; E-mail: gadiaz@ciq.uchile.cl.

Word count: 6374 words

Abstract

Aims: Despite the pharmacological arsenal to treat hypertension, chronic patients may develop irreversible cardiac remodeling and fibrosis. As Resolvin-D1 (RvD1) elicits potent anti-inflammatory and pro-resolving effects in various pathological models, we set to evaluate these effects in an Angiotensin (Ang-II) hypertension model.

Methods and results: Alzet® osmotic mini-pumps filled with Ang-II (1.5 mg/kg/day) were implanted in C57BL/6 mice for 7 or 14 days, RvD1 (3 µg/kg/day, i.p) was administered one day after the surgery and during the infusion period. Blood pressure and functional parameters were assessed by echocardiography. At the end of the experimental schemes, tissues were harvested and histological parameters were studied. RvD1 ameliorated at 7 and 14 days Ang-II induced neutrophil and monocyte infiltration; ICAM-1 and VCAM-1 expression; IL-1β, TNF-α, IL-6, KC, MCP-1 plasmatic levels while increasing IL-10; cardiac hypertrophy, interstitial and perivascular fibrosis, and hypertension.

Conclusions: This study unveils novel cardioprotective effects of RvD1 in Ang-II-induced hypertension and cardiac remodeling, giving insights of a potential clinical application.

Word count: 160

Translational Perspective: Recent evidence points to unresolved inflammation as responsible of perpetuating chronic diseases with worse outcomes. In this study we determined the effects of RvD1, an anti-inflammatory and pro-resolution molecule, in an Ang-II model of hypertension caused by exacerbated inflammation and cardiac remodeling. RvD1 attenuated the inflammatory response in cardiac tissue and plasma, reduced LV hypertrophy and collagen deposition, and partially prevented systolic and diastolic hypertension. These findings sustain the potential role of RvD1 as a coadjutant therapy in patients with chronic hypertension.

Word count: 84

1 Introduction

High blood pressure (HBP) is one of the most prevalent non-communicable diseases in the world, where 28% of the population could suffer from it without even being aware of its existence, thus giving high priority to related research considering the physiological long-term consequences and health system overload¹. Among the main triggers of arterial hypertension are cellular aging, metabolic diseases and hormonal dysregulation². It is in the latter context that the renin-angiotensin-aldosterone system (RAAS) and its main effector molecule, Angiotensin II (Ang-II), has a fundamental role.

Ang-II is the main hormone in the RAAS system and has endocrine, paracrine and autocrine functions that regulates both the volume of circulating plasma by increasing the reabsorption of sodium and water at the renal level, and activation of local inflammatory mechanisms³. Moreover, Ang-II exerts its effects through the AT1 receptor, promoting cardiomyocyte (CM) hypertrophy, expression of growth factors (e.g TGF- β), pro-inflammatory chemokines (e.g IL-1 β and MCP-1) and components of the extracellular matrix (ECM) such as collagen I and fibronectin in cardiac fibroblasts (CF), and nitric oxide synthase uncoupling along with enhanced expression of ICAM-1, VCAM-1 and selectins in endothelial cells⁴. Therefore, Ang-II has been shown to increase leukocyte infiltration, adhesion, and migration in the aorta, heart, brain, and kidneys, leading to elevated levels of inflammatory cytokines and increased blood pressure (BP)⁵. Additionally, macrophages express the AT1 receptor, which, when activated by Ang-II, induces macrophage differentiation to the M2 phenotype⁶ and in murine models that do not produce mature B and T lymphocytes, Ang-II infusion does not generate an increase in blood pressure⁷. These antecedents provide evidence for the existing cross

communication between Ang-II, inflammation, the development of HBP and subsequent cardiac remodeling, an initial adaptive response of the heart to compensate for the increase in left ventricular (LV) pressure due to hemodynamic overload⁸.

The denominated specialized pro-resolving mediators (SPM) are a family of molecules that have omega-3 fatty acids as precursors. In the case of Resolvin-D1 (RvD1), it is endogenously synthesized from docosahexaenoic acid (DHA) at the site of inflammation due to interactions between leukocytes and local tissue⁹, exerting anti-inflammatory actions through its receptor FPR2/ALX such as decreased levels of TNF- α , IL-1 β , MCP-1¹⁰ and neutrophil migration, together with pro-resolutive actions such as increased non-phlogistic monocyte recruitment, increased phagocytic capacity and macrophage differentiation from M1 to M2¹¹. There are few studies where the effect of RvD1 has been studied in cardiac tissue, but it has been shown that in models of myocardial infarction RvD1 promotes the synthesis of the ALX receptor, neutrophil efferocytosis associated with an increase in the M2 macrophage population, and the decrease in collagen deposition¹². Furthermore, in an I/R model, RvD1 prevented CM apoptosis by decreasing activation of caspase 3/8 and NF- κ B, along with activation of the Pi3K/AKT pathway¹³.

Due to these antecedents, it is of interest to study whether RvD1, due to its anti-inflammatory and pro-resolution actions, is able to limit the inflammatory effect of Ang-II associated with the development of HBP and cardiac hypertrophy, and therefore providing novel and promising cardioprotective effects.

44

45

2 Materials and methods

2.1 Animals

Male C57BL/6 mice between 6-8 weeks old and 20-24 g were obtained from the animal breeding facility of the Faculty of Dentistry of the University of Chile. The animals were identified with ear tags and kept in cages separated by experimental group (at a maximum of three animals per cage) with light/dark cycles of 12 h and free access to food and water. All studies were carried out in compliance with the Institutional Committee for the Care and Use of Animals of the University of Chile (FOUCH 130806), ARRIVE guidelines and NIH Guide for the Care and Use of Laboratory Animals, updated in 2011 (<http://grants.nih.gov/grants/olaw/Guide-for-the-Care-and-Use-of-Laboratory-Animals>)

2.2 Ang-II hypertension model

Osmotic pumps (Alzet, model 1007D or 1002) were filled with saline diluted Ang-II (A9525, Sigma-Aldrich) followed by priming according to manufacturer instructions. RvD1 (#10012554, Cayman Chemical) was prepared with saline and stored at -80°C until use.

In an aseptic condition, mice were anesthetized with oxygen and isoflurane (2-3%) during the pump implant procedure (10-15 minutes). First, mice were given ophthalmic ointment and s.c analgesic injection (meloxicam 2 mg/kg), then a small mid-scapular incision was made and a subcutaneous pocket was created using a hemostat. Subsequently, the osmotic pump was inserted and the incision was closed with sutures. After the surgery, mice received s.c fluid therapy, antiseptic wound ointment and were allowed to wake up and put back in their cage. For sham-treated mice, the subcutaneous pocket was closed

without implanting a pump. Mice were infused with Angiotensin-II (1.5 mg/kg/day) for 7 or 14 days¹⁴, and saline or Resolvin-D1 (3 ug/kg/day i.p)¹² was administered daily starting one day after the surgery and until being euthanized.

The animals were randomized to their respective groups based on body weight, resulting in 8 experimental groups: 1) Control (sham) 7 days, 2) Control (sham) 14 days, 3) Ang-II infusion 7 days, 4) Ang-II infusion 14 days, 5) RvD1 7 days, 6) RvD1 14 days, 7) Ang-II infusion + RvD1 7 days, 8) Ang-II infusion + RvD1 14 days. 6 animals were assigned to each group, and a total of 55 animals were utilized in the study, taking into account the model and tissue extraction setup, 3 animals that died after the surgery and 1 animal that died due to fighting with its littermates.

2.3 Echocardiography

One week prior to the pump implantation, mice were trained to undergo the procedure (every other day the animals were handled imitating the exam while spreading gel in their thorax with a mock transducer). The day before the surgery, 2D transthoracic echocardiography (Vivid Q, GE Healthcare) was performed to assess basal cardiac dimensional and functional parameters without anesthesia, as described¹⁵. Interventricular septal wall thickness (IVWST), posterior wall thickness (PWT), left ventricular end-diastolic and end-systolic diameters (LVEDd and LVESd), ejection fraction (EF) and fractional shortening (FS) were measured. The same procedure was repeated at 14 days of Ang-II delivery.

2.4 Blood pressure measurement

The tail-cuff method (NIBP LE5001, Harvard Apparatus) was utilized as previously described¹⁶. One week before the pump implantation and every other day when not performing echo training, mice were acclimatized to the restraint holder for 10 minutes and then allowed to go back to their cages. The day before the surgery, mice were restrained in the holder and their tails were warmed on a warming pad for 20 minutes before starting an initial cycle of 30 basal systolic (SAP), diastolic (DAP), and mean blood pressure (MAP) along with heart frequency (BPM) measurements. An average of 15-20 acceptable measurements was recorded for each mouse. This procedure was repeated at 7 and 14 days of Ang-II infusion.

2.5 Tissue harvest and HW/TL ratio

Animals were administrated i.p ketamine/xylazine cocktail (87.5/12.5 mg/kg, 0.1 ml per 20 g mouse) and the level of anesthesia was assessed by pedal reflex. Blood was collected by retro-orbital puncture in EDTA 0.5 M coated tubes, after which the thoracic cavity was cleaved altogether with the diaphragm and the heart was excised, weighted, photographed and then fixed in 4% neutral buffered formalin. The right tibia was dissected, cleaned and measured with a ruler to calculate the heart weight/tibia length (HW/TL) ratio.

2.6 Immunohistochemistry

Hearts were processed and prepared following previously validated protocols¹⁶. Paraffin embedded tissues were cut into 5 µm sections for histological analyses. To investigate infiltration tissue formation, hematoxylin/eosin (HE) staining was used. To determinate the collagen positive area, Masson trichrome staining was performed followed by analysis using ImageJ software as described¹⁶. For each sample, 5 random fields at 40X were captured using a light microscope (Leica DM500, Leica Microsystems), measured and averaged for each mouse. To study the magnitude of inflammation, tissue slides were incubated with primary antibodies against CD68 (Ab125212, Abcam, 1:200), MPO (sc-390109, Santa Cruz Biotechnology, 1:50), ICAM-1 (Ab222736, Abcam, 1:200), and VCAM (Ab134047, Abcam, 1:200) for 1.5 h at room temperature and then detected utilizing Novolink Polymer Detection System (Leica Biosystems). As with the previous staining, 5 random fields were taken at 40X, measured and averaged per animal. The DAB positive area was measured by densitometry as reported¹⁷. Fiji software was used for all analyses¹⁸.

2.7 Immunofluorescence

Cardiomyocyte cross sectional area (CSA) was determined with FITC-conjugated wheat germ agglutinin (WGA)¹⁶. For each sample, 5 random fields were taken at digital 40X using a ZOE Fluorescent Imager (Biorad), then 20-30 cardiomyocytes per capture were measured utilizing Fiji software. The observer was blinded to the experimental conditions.

2.8 Plasma sampling for Multiplex assay

Plasma was separated by centrifugation of collected blood at 3000 rpm for 15 min and 4°C without using brakes, then stored in a deep freezer (-80°C). Plasma levels of TNF-alpha, IL-1beta, IL-6, IL-10, KC and MCP-1 were determined using a custom Multiplex kit (MCYTOMAG-70K, Merck Millipore) according to manufacturer instructions.

2.9 Statistical analysis

All values plotted are presented as means \pm standard deviation (SD) of 6 mouse per experimental condition. Data distribution was determined with the Shapiro-Wilk test of normality. To perform multi-group comparison, one-way ANOVA followed by Tukey test was used and respective p-values are shown in each chart. All possible pairwise comparisons were performed and no animals were excluded from the study. The representative images shown represent the average data obtained in all samples. All statistical analyses were performed using GraphPad Prism version 9.0.2.

3. Results

3.1 RvD1 suppresses neutrophil and monocyte infiltration in cardiac tissue

During acute cardiac inflammation, leukocytes are recruited to clear the injured tissue and initiate tissue repair, as seen in Ang-II infusion models¹⁹. In our study, Ang-II delivery resulted in a marked increase of granulation tissue presence (Figure 1A), neutrophil (Figure 2B) and monocyte infiltration (Figure 2C) at 7 and 14 days, with more intensity at 1 week of infusion (FALTAN LOS MONOCITOS) and specially focused in the perivascular area. Notably, the treatment with RvD1 prevented Ang-II induced inflammation evidenced in reduced granulation tissue formation and leukocyte infiltration.

3.2 RvD1 decreases cardiac VCAM-1 and ICAM-1 levels

Following with the previous idea, ICAM-1 and VCAM-1 have an essential role in the adhesion and activation of leukocytes in inflammatory events²⁰, thus we studied the presence of these proteins by IHC. Ang-II infusion elicited a steep elevation of ICAM-1 (Figure 2A) and VCAM-1 (Figure 2B) staining in the heart tissue to a greater degree at 14 days for ICAM-1 and mostly around vessels than in the interstitial area. However, the treatment with RvD1 was able to decrease the Ang-II enhanced levels of VCAM-1 and ICAM-1 at both infusion schemes (Figure 2C).

3.3 RvD1 reduces circulating pro-inflammatory cytokines

It has been described that Ang-II alters systemic and local levels of pro-inflammatory and anti-inflammatory cytokines²¹. To have a better understanding of the systemic inflammatory process, we investigated the level of plasmatic cytokines. Ang-II increased the plasma concentration of the pro-inflammatory cytokines IL-1 β , TNF- α , IL-6, KC and MCP-1, evidenced with greater magnitude at 7 days IL-6, KC and MCP-1, and at 14 days of Ang-II infusion for TNF- α and IL-1 β , with similar levels at both delivery times. RvD1 treatment significantly decreased the presence of all pro-inflammatory cytokines. On the other hand, Ang-II decreased plasmatic IL-10 at 7 and 14 days evidenced in a minor downward trend; and more importantly, the administration of RvD1 triggered a steep increase of IL-10 at 7 days and even more at 14 days (Figure 3), not seen in the RvD1-only group.

3.4 RvD1 partially prevents cardiac hypertrophy

Cardiac hypertrophy results from increased CM size partly as a response to the increased overload, and most importantly, to the direct hypertrophic actions of Ang-II on CM via enhanced TGF- β 1 secretion by CF²². In our study, we aimed to evaluate the protective effects of RvD1 in the development of this pathology. As depicted in the Figure 4A, hearts from the Ang-II group visually appear enlarged, while the animals treated with RvD1 have smaller hearts yet still hypertrophied compared to the control group. This is further confirmed with higher HW/TL ratio in the Ang-II group at 7 and 14 days, higher at 14 days and partially reversed in the Ang-II+RvD1 animals (Figure 4B). Furthermore, WGA-stained CM have remarkably increased CSA at 7 and even more at 14 days, while Ang-

195 II+RvD1 treated mice exhibit CM with decreased area, but still enlarged in comparison to
196 the control group.

198 **3.5 RvD1 restores cardiac functional parameters**

199 In Ang-II-induced hypertension, the LV wall thickening and cardiac remodeling triggers
200 diastolic dysfunction that can progress to decreased LV filling and heart failure (HF) with
201 preserved EF²³. Due to the clinical relevance of this pathology, a thorough study of
202 cardiac functional parameters was realized. Whereas Ang-II infused mice evidenced a
203 thicker septum and posterior wall (Figure 5A) and systolic/diastolic dysfunction evidenced
204 in shorter LVESd and LVEDd, RvD1 rescued the cardiac functionality by partially
205 preventing IWT and PWT hypertrophy and LV diameter changes (Figure 5B). Of
206 importance, even though Ang-II disrupted LVESd and LVEDd, the EF and FS were
207 preserved in all experimental groups.

209 **3.6 RvD1 partially decreases cardiac collagen deposition**

210 Patients with HBP develop changes in their LV that lead to structural remodeling of the
211 myocardium, as oxidative stress and fibrosis. The altered balance between the synthesis
212 and degradation of collagen I/III molecules ends with excessive deposition of collagen
213 fibers in the myocardium with impaired compliance and contractibility¹. In our model, Ang-
214 II increases collagen deposition at 7 (Figure 6A) and 14 (Figure 6B) days of infusion
215 evidenced in deeper Masson's trichrome staining. This is appreciated in interstitial and
216 specially in perivascular tissue, with a significative difference in the latter at two weeks of

Ang-II delivery (Figure 6C). Notably, RvD1 again exerts a cardioprotective effect by partially preventing perivascular and interstitial collagen deposition, compared to both Ang-II groups.

3.7 RvD1 attenuates HBP development

Ang-II raises blood pressure by various actions, importantly pro-inflammatory effects in heart tissue and vessels, along with pro-fibrotic effects in vascular smooth muscle cells and fibroblasts²¹. As an endpoint of our model, we assessed the variation in blood pressure (BP) at 7 and 14 days of infusion. We demonstrated that, effectively, Ang-II increases SAP (Figure 7A), DAP (Figure 7B), MAP and BPM (Figure 7C) at both experimental periods, with greater HBP at 2 weeks. Nonetheless, RvD1 attenuated the HBP increment elicited by Ang-II, at 7 and 14 days.

4. Discussion

In the present study, we investigated the cardioprotective actions of RvD1 in four mayor Ang-II-induced outcomes: cardiac inflammation evidenced in neutrophil and monocyte infiltration, in conjunction with ICAM-1 and VCAM-1 expression, and circulating pro-inflammatory cytokines levels; cardiac remodeling manifested in heart weight, CM hypertrophy, LV thickening and alteration of functional parameters; finalizing with systolic and diastolic blood pressure increase.

4.1 Anti-inflammatory actions of RvD1

Ang-II exerts important pro-inflammatory actions in cardiovascular diseases triggering vascular damage, cellular adhesion molecules expression, cytokine secretion and immune cells recruitment ²¹. We show that Ang-II at 7 and 14 days induces granulation tissue formation, composed of infiltrating leukocytes, proliferating CF and collagen in a late phase. In acute inflammation, Ang-II increases vascular permeability through endothelial VEGF synthesis that, orchestrated with enhanced expression of ICAM-1, VCAM-1 and KC, facilitates neutrophil infiltration to the cardiac tissue ³. Paracrine chemokine secretion and Angi-II-mediated ROS damage contributes to maintain the inflammatory microenvironment. Afterwards, neutrophil apoptosis and MCP-1 secretion by CF and CM, attracts monocyte subpopulations to the injury zone and subsequent differentiation to M1 macrophages in response to inflammatory cytokines as IL-6 ²⁴. This process is usually self-limited, nonetheless, chronic Ang-II infusion elicits permanent myocardial damage evidenced in uncontrolled collagen deposition and enhanced

expression of IL-6, IL-1 β and MCP-1, favoring cardiac remodeling. In our study, the peak neutrophil and monocyte presence was seen at 7 days, a more acute than chronic inflammation stage, even though Wang et. al demonstrated leukocyte infiltration starting one day after Ang-II infusion ²⁵ and reaching its maximum at 14 days. However, at 14 days we evidenced a statistically significant decrease in neutrophil and monocyte infiltration, that may be product of pro-resolutive mechanisms initiated in the cardiac tissue ¹². Interestingly, RvD1 blunted neutrophil and monocyte presence at 7 and 14 days, exerting anti-inflammatory and pro-resolutive actions. Kain et. al ¹² demonstrated in a myocardial infarct model that RvD1 decreased neutrophil infiltration by reducing spleen neutrophil density, while Spinoza et. al showed that RvD1 decreases aortic aneurism formation by inhibiting NETosis²⁶. Whether those mechanisms are involved in Ang-II-dependent inflammation is unknown.

As stated before, Ang-II infusion also triggers ICAM-1 and VCAM-1 expression, seen at 14 days of delivery and contributing the infiltration of leukocytes with posterior cardiovascular damage ²⁷. Our data supports this idea, finding enhanced interstitial and particularly perivascular ICAM-1 and VCAM-1 expression at 7 and 14 days, even greater at the latter period for ICAM-1 and pointing to a major endothelial involvement and time-dependent effect of Ang-II in the expression of this molecule ²⁸. Notably, RvD1 was able to prevent ICAM-1 and VCAM-1 expression in accordance to our previous findings in rat CF stimulated with LPS ²⁹ and imiquimod-induced psoriasiform dermatitis ³⁰.

Pro-inflammatory actions of Ang-II also involve cytokine expression and secretion locally and systemically ²¹, seen previously in increased IL-1 β , IL-6, TNF- α , KC and MCP-1 mRNA levels in heart ²⁵ and monocytes culture media, with consequent M1 polarization³¹.

In this study, Ang-II elicited a greater increase in plasmatic IL-6, KC and MCP-1 at 7 rather than 14 days indicating an acute inflammatory phase dominated by recruiting signals³, and vice versa with IL-1 β and TNF- α . Our data supports systemic anti-inflammatory actions of RvD1 by decreasing plasmatic levels of IL-1 β , IL-6, TNF- α , KC and MCP-1 at 7 and 14 days, demonstrated beforehand in arthritis³² and pancreatic injury models³³. The correlation of plasmatic and cardiac tissue cytokine levels was not determined. Although IL-10 levels were not affected by Ang-II, RvD1 treatment sharply increased its plasma concentration at 7 and even more at 14 days, demonstrating anti-inflammatory and pro-resolutive actions in presence of inflammatory stimuli^{12,32}. Whether this is related to enhanced anti-inflammatory M2 macrophage polarization, it was not studied.

4.2 RvD1 prevents Ang-II-induced cardiac remodeling

Chronic hypertension generates changes in the heart architecture, evidenced in CM hypertrophy, interstitial and perivascular fibrosis and LV thickening. Cardiac remodeling is a detrimental process that can decrease cardiac function and lead to heart failure (HF), thus is a desirable clinical target for therapy given the direct relation between LV hypertrophy and worsening of long-term outcomes, even more evident when risks factors as obesity and age may coexist with hypertension³⁴. Ang-II, by inducing pressure overload and inflammatory mechanisms in heart tissue, contributes to an initial adaptative response, characterized by concentric hypertrophy and LV thickening. Sustained activation of these mechanisms leads to pathological hypertrophy by activation of fibrotic pathways linked to CM death, CF differentiation and excessive collagen deposition⁴.

In this context, Ang-II infusion at 7 and 14 days increased heart mass and CM area with enhanced hypertrophic effects at 2 weeks of Ang-II delivery. Furthermore, echocardiographic evaluation showed LV thickening, in addition to systolic and diastolic dysfunction according to LV diameter, but preserved EF as seen in patients with heart failure and preserved ejection fraction (HFpEF)³⁵. On the other hand, daily RvD1 administration partially prevented cardiac hypertrophy at both infusion schemes. Kain et. al demonstrated RvD1 antihypertrophic properties in myocardial infarction expressed in decreased PWT thickening, HW/TL ratio¹² and CM hypertrophy³⁶; and similar effects were evidenced in epidermal hypertrophy within a model of skin inflammation³⁷.

Regarding cardiac fibrosis, through Masson's trichrome we demonstrated increasing collagen deposition at 7 and 14 days, as extensively described¹. Of importance, RvD1 prevented collagen deposition at the interstitial and perivascular area. Wang et. al²⁵ demonstrated essential CXCL1/KC participation in Ang-II induced fibrosis, while Matsuda et. al¹⁹ evaluated the MCP-1 axis. Recapitulating our current findings, RvD1 decreased plasmatic levels of KC and MCP-1, therefore it may be certain relation between both events that needs to be further investigated. However, as far as our review of the literature covers there are not studies that explored the antihypertrophic and antifibrotic actions of RvD1 in Ang-II induced cardiac remodeling, therefore giving our results remarked novelty.

4.3 Antihypertensive effects of RvD1 in Ang-II infusion

In this study we show for the first time that RvD1 attenuates the Ang-II-induced increase of SAP, DAP, MAP and BPM at 7 and 14 days, without reaching a maximum value at two

weeks of infusion. Previously, there only were studies that investigated the role of dietary supplement of n-3 polyunsaturated fatty acid (n-3 PUFAs) in mice ³⁸ and adults ³⁹, where there was found a minor downward trend in SBP.

Recently, it has been described the close relation between inflammation and regulation of hypertension. Ang-II induced hypertension is blunted in mice with deficiency of mature T and B lymphocytes, macrophages, or lysozyme M-positive monocytes ⁷. Similar results has been seen in mice with inhibition of MCP-1 ⁴⁰, TNF- α ⁴¹, IL-6⁴² and ICAM-1²⁸. In this respect, the anti-inflammatory effects of RvD1 comprehending lymphocyte and cytokine regulation have been reviewed extensively elsewhere¹⁰ and importantly, has been demonstrated in this study. Hence, the described antihypertensive effect of RvD1 may partly be due limited neutrophil and monocyte infiltration in cardiac tissue, decreased pro-inflammatory plasmatic cytokines, and enhanced circulating expression of IL-10, as seen in an IL-10 KO model ⁴³. However, we cannot rule out the role of vessels and kidney in the genesis of HBP, key regulators of circulating plasma and the RAAS system.

4.4 Limitations

The main limitation of this study is that, although we showed clear anti-inflammatory, anti-hypertensive, anti-hypertrophic and anti-fibrotic effects of RvD1, we did not further investigate the underlying mechanisms directing those actions. Nonetheless, other groups have demonstrated effects of RvD1 suppressing NF- κ B while enhancing the PI3K-AKT and MEK-ERK transductional pathways in different pathological models ¹⁰. It remains

to be elucidated the exact mechanisms regulating RvD1 effects in Ang-II induced hypertension through *in vivo* and *in vitro* assays.

5. Conclusions

RvD1 ameliorated at 7 and 14 days Ang-II induced neutrophil and monocyte infiltration; ICAM-1 and VCAM-1 expression; IL-1 β , TNF- α , IL-6, KC, MCP-1 plasmatic levels while increasing IL-10; cardiac hypertrophy, fibrosis and hypertension. These results suggest cardioprotective effects that may be applied in clinical practice.

5.1 Acknowledgements

We thank Ana María Silva Rozas for her unconditional support, Natalie de la Jara together with David Silva for their IHC technical assistance, and Eliana Pino along Valeria Garrido for their assistance with the *in vivo* model.

5.2 Source of funding

This work was supported by FONDECYT grant 1170425 from Agencia Nacional de Investigación y Desarrollo de Chile (ANID) to G.D.A, and ANID Scholarship Program/DOCTORADO BECAS CHILE/2017-21170177 to F.O.S.

5.3 Conflict of interest

All authors have declared that no conflict of interest exists.

5.4 Statement of contributions

F.O.S, G.D.A, C.P and C.S.F conceived the study and study design. F.O.S performed all the experiments, interpreted results and wrote the manuscript. N.D.G helped with the animal experiments. J.E.C assisted with the statistical analysis. G.D.A and S.L edited the manuscript. C.E, R.V and J.M.O provided essential insights to the manuscript.

5.5 Data availability statement

The data underlying this article will be shared on reasonable request to the corresponding author.

6. References (no olvidar cambiar al formato del journal)

- (1) Smolgovsky, S.; Ibeh, U.; Tamayo, T. P.; Alcaide, P. Adding Insult to Injury - Inflammation at the Heart of Cardiac Fibrosis. *Cell Signal* **2021**, *77*, 109828. <https://doi.org/10.1016/j.cellsig.2020.109828>.
- (2) Wang, L.; Szklo, M.; Folsom, A. R.; Cook, N. R.; Gapstur, S. M.; Ouyang, P. ENDOGENOUS SEX HORMONES, BLOOD PRESSURE CHANGE, AND RISK OF HYPERTENSION IN POSTMENOPAUSAL WOMEN: THE MULTI-ETHNIC STUDY OF ATHEROSCLEROSIS. *Atherosclerosis* **2012**, *224* (1), 228–234. <https://doi.org/10.1016/j.atherosclerosis.2012.07.005>.
- (3) Montezano, A. C.; Nguyen Dinh Cat, A.; Rios, F. J.; Touyz, R. M. Angiotensin II and Vascular Injury. *Curr. Hypertens. Rep.* **2014**, *16* (6), 431. <https://doi.org/10.1007/s11906-014-0431-2>.
- (4) Kong, P.; Christia, P.; Frangogiannis, N. G. The Pathogenesis of Cardiac Fibrosis. *Cell. Mol. Life Sci.* **2014**, *71* (4), 549–574. <https://doi.org/10.1007/s00018-013-1349-6>.
- (5) Restini, C. B. A.; Garcia, A. F. E.; Natalin, H. M.; Natalin, G. M.; Rizzi, E. Signaling Pathways of Cardiac Remodeling Related to Angiotensin II. *Renin-Angiotensin System - Past, Present and Future* **2017**. <https://doi.org/10.5772/66076>.
- (6) Aki, K.; Shimizu, A.; Masuda, Y.; Kuwahara, N.; Arai, T.; Ishikawa, A.; Fujita, E.; Mii, A.; Natori, Y.; Fukunaga, Y.; Fukuda, Y. ANG II Receptor Blockade Enhances Anti-Inflammatory Macrophages in Anti-Glomerular Basement Membrane Glomerulonephritis. *Am. J. Physiol. Renal Physiol.* **2010**, *298* (4), F870-882. <https://doi.org/10.1152/ajprenal.00374.2009>.

- (7) Guzik, T. J.; Hoch, N. E.; Brown, K. A.; McCann, L. A.; Rahman, A.; Dikalov, S.; Goronzy, J.; Weyand, C.; Harrison, D. G. Role of the T Cell in the Genesis of Angiotensin II Induced Hypertension and Vascular Dysfunction. *J. Exp. Med.* **2007**, *204* (10), 2449–2460. <https://doi.org/10.1084/jem.20070657>.
- (8) Nakamura, M.; Sadoshima, J. Mechanisms of Physiological and Pathological Cardiac Hypertrophy. *Nat Rev Cardiol* **2018**, *15* (7), 387–407. <https://doi.org/10.1038/s41569-018-0007-y>.
- (9) Dalli, J.; Serhan, C. N. Identification and Structure Elucidation of the Pro-Resolving Mediators Provides Novel Leads for Resolution Pharmacology. *Br. J. Pharmacol.* **2019**, *176* (8), 1024–1037. <https://doi.org/10.1111/bph.14336>.
- (10) Serhan, C. N.; Levy, B. D. Resolvins in Inflammation: Emergence of the pro-Resolving Superfamily of Mediators. *J. Clin. Invest.* **2018**, *128* (7), 2657–2669. <https://doi.org/10.1172/JCI97943>.
- (11) Capó, X.; Martorell, M.; Busquets-Cortés, C.; Tejada, S.; Tur, J. A.; Pons, A.; Sureda, A. Resolvins as Proresolving Inflammatory Mediators in Cardiovascular Disease. *Eur J Med Chem* **2018**, *153*, 123–130. <https://doi.org/10.1016/j.ejmech.2017.07.018>.
- (12) Kain, V.; Ingle, K. A.; Colas, R. A.; Dalli, J.; Prabhu, S. D.; Serhan, C. N.; Joshi, M.; Halade, G. V. Resolvin D1 Activates the Inflammation Resolving Response at Splenic and Ventricular Site Following Myocardial Infarction Leading to Improved Ventricular Function. *J. Mol. Cell. Cardiol.* **2015**, *84*, 24–35. <https://doi.org/10.1016/j.yjmcc.2015.04.003>.

- 431 (13) Gilbert, K.; Bernier, J.; Bourque-Riel, V.; Malick, M.; Rousseau, G. Resolvin D1
432 Reduces Infarct Size Through a Phosphoinositide 3-Kinase/Protein Kinase B
433 Mechanism. *J. Cardiovasc. Pharmacol.* **2015**, *66* (1), 72–79.
434 <https://doi.org/10.1097/FJC.0000000000000245>.
- 435 (14) Atchison, D. K.; O'Connor, C. L.; Menon, R.; Otto, E. A.; Ganesh, S. K.; Wiggins,
436 R. C.; Smrcka, A. V.; Bitzer, M. Hypertension Induces Glomerulosclerosis in
437 Phospholipase C-E1 Deficiency. *Am J Physiol Renal Physiol* **2020**, *318* (5), F1177–
438 F1187. <https://doi.org/10.1152/ajprenal.00541.2019>.
- 439 (15) Battiprolu, P. K.; Hojaye, B.; Jiang, N.; Wang, Z. V.; Luo, X.; Iglewski, M.; Shelton,
440 J. M.; Gerard, R. D.; Rothermel, B. A.; Gillette, T. G.; Lavandero, S.; Hill, J. A.
441 Metabolic Stress-Induced Activation of FoxO1 Triggers Diabetic Cardiomyopathy in
442 Mice. *J Clin Invest* **2012**, *122* (3), 1109–1118. <https://doi.org/10.1172/JCI60329>.
- 443 (16) Schiattarella, G. G.; Altamirano, F.; Tong, D.; French, K. M.; Villalobos, E.; Kim, S.
444 Y.; Luo, X.; Jiang, N.; May, H. I.; Wang, Z. V.; Hill, T. M.; Mammen, P. P. A.; Huang,
445 J.; Lee, D. I.; Hahn, V. S.; Sharma, K.; Kass, D. A.; Lavandero, S.; Gillette, T. G.;
446 Hill, J. A. Nitrosative Stress Drives Heart Failure with Preserved Ejection Fraction.
447 *Nature* **2019**, *568* (7752), 351–356. <https://doi.org/10.1038/s41586-019-1100-z>.
- 448 (17) Qu, X.; Zhang, X.; Yao, J.; Song, J.; Nikolic-Paterson, D. J.; Li, J. Resolvins E1 and
449 D1 Inhibit Interstitial Fibrosis in the Obstructed Kidney via Inhibition of Local
450 Fibroblast Proliferation. *J. Pathol.* **2012**, *228* (4), 506–519.
451 <https://doi.org/10.1002/path.4050>.
- 452 (18) Schindelin, J.; Arganda-Carreras, I.; Frise, E.; Kaynig, V.; Longair, M.; Pietzsch, T.;
453 Preibisch, S.; Rueden, C.; Saalfeld, S.; Schmid, B.; Tinevez, J.-Y.; White, D. J.;

Hartenstein, V.; Eliceiri, K.; Tomancak, P.; Cardona, A. Fiji: An Open-Source Platform for Biological-Image Analysis. *Nature Methods* **2012**, *9* (7), 676–682. <https://doi.org/10.1038/nmeth.2019>.

(19) Matsuda, S.; Umemoto, S.; Yoshimura, K.; Itoh, S.; Murata, T.; Fukai, T.; Matsuzaki, M. Angiotensin II Activates MCP-1 and Induces Cardiac Hypertrophy and Dysfunction via Toll-like Receptor 4. *J. Atheroscler. Thromb.* **2015**, *22* (8), 833–844. <https://doi.org/10.5551/jat.27292>.

(20) Olivares-Silva, F.; Landaeta, R.; Aránguiz, P.; Bolivar, S.; Humeres, C.; Anfossi, R.; Vivar, R.; Boza, P.; Muñoz, C.; Pardo-Jiménez, V.; Peiró, C.; Sánchez-Ferrer, C. F.; Díaz-Araya, G. Heparan Sulfate Potentiates Leukocyte Adhesion on Cardiac Fibroblast by Enhancing Vcam-1 and Icam-1 Expression. *Biochim Biophys Acta Mol Basis Dis* **2018**, *1864* (3), 831–842. <https://doi.org/10.1016/j.bbadis.2017.12.002>.

(21) Satou, R.; Penrose, H.; Navar, L. G. Inflammation as a Regulator of the Renin-Angiotensin System and Blood Pressure. *Curr. Hypertens. Rep.* **2018**, *20* (12), 100. <https://doi.org/10.1007/s11906-018-0900-0>.

(22) Kurdi, M.; Booz, G. W. NEW TAKE ON THE ROLE OF ANGIOTENSIN II IN CARDIAC HYPERTROPHY AND FIBROSIS. *Hypertension* **2011**, *57* (6), 1034–1038. <https://doi.org/10.1161/HYPERTENSIONAHA.111.172700>.

(23) Yoon, S.; Eom, G. H. Heart Failure with Preserved Ejection Fraction: Present Status and Future Directions. *Experimental & Molecular Medicine* **2019**, *51* (12), 1–9. <https://doi.org/10.1038/s12276-019-0323-2>.

- (24) Fontes, J. A.; Rose, N. R.; Čiháková, D. The Varying Faces of IL-6: From Cardiac Protection to Cardiac Failure. *Cytokine* **2015**, *74* (1), 62–68. <https://doi.org/10.1016/j.cyto.2014.12.024>.
- (25) Wang, L.; Zhang, Y.-L.; Lin, Q.-Y.; Liu, Y.; Guan, X.-M.; Ma, X.-L.; Cao, H.-J.; Liu, Y.; Bai, J.; Xia, Y.-L.; Du, J.; Li, H.-H. CXCL1-CXCR2 Axis Mediates Angiotensin II-Induced Cardiac Hypertrophy and Remodelling through Regulation of Monocyte Infiltration. *Eur. Heart J.* **2018**, *39* (20), 1818–1831. <https://doi.org/10.1093/eurheartj/ehy085>.
- (26) Spinosa, M.; Su, G.; Salmon, M. D.; Lu, G.; Cullen, J. M.; Fashandi, A. Z.; Hawkins, R. B.; Montgomery, W.; Meher, A. K.; Conte, M. S.; Sharma, A. K.; Ailawadi, G.; Upchurch, G. R. Resolvin D1 Decreases Abdominal Aortic Aneurysm Formation by Inhibiting NETosis in a Mouse Model. *J Vasc Surg* **2018**, *68* (6S), 93S–103S. <https://doi.org/10.1016/j.jvs.2018.05.253>.
- (27) Lin, Q.-Y.; Lang, P.-P.; Zhang, Y.-L.; Yang, X.-L.; Xia, Y.-L.; Bai, J.; Li, H.-H. Pharmacological Blockage of ICAM-1 Improves Angiotensin II-Induced Cardiac Remodeling by Inhibiting Adhesion of LFA-1⁺ Monocytes. *American Journal of Physiology-Heart and Circulatory Physiology* **2019**, *317* (6), H1301–H1311. <https://doi.org/10.1152/ajpheart.00566.2019>.
- (28) Kiarash Arash; Pagano Patrick J.; Tayeh Mahmoud; Rhaleb Nour-Eddine; Carretero Oscar A. Upregulated Expression of Rat Heart Intercellular Adhesion Molecule-1 in Angiotensin II– but Not Phenylephrine- Induced Hypertension. *Hypertension* **2001**, *37* (1), 58–65. <https://doi.org/10.1161/01.HYP.37.1.58>.

- (29) Salas-Hernández, A.; Espinoza, C.; Vivar, R.; Espitia Corredor, J.; Lillo, J.; Parra-Flores, P.; Sánchez-Ferrer, C.; Peiró, C.; Diaz-Araya, G. Resolvin D1 and E1 Promote Resolution of Inflammation in Rat Cardiac Fibroblast in Vitro. *Molecular Biology Reports* **2021**, *48*. <https://doi.org/10.1007/s11033-020-06133-8>.
- (30) Xu, J.; Duan, X.; Hu, F.; Poorun, D.; Liu, X.; Wang, X.; Zhang, S.; Gan, L.; He, M.; Zhu, K.; Ming, Z.; Chen, H. Resolvin D1 Attenuates Imiquimod-Induced Mice Psoriasiform Dermatitis through MAPKs and NF- κ B Pathways. *Journal of Dermatological Science* **2018**, *89* (2), 127–135. <https://doi.org/10.1016/j.jdermsci.2017.10.016>.
- (31) Wu, L.; Chen, K.; Xiao, J.; Xin, J.; Zhang, L.; Li, X.; Li, L.; Si, J.; Wang, L.; Ma, K. Angiotensin II Induces RAW264.7 Macrophage Polarization to the M1-type through the Connexin 43/NF- κ B Pathway. *Molecular Medicine Reports* **2020**, *21* (5), 2103–2112. <https://doi.org/10.3892/mmr.2020.11023>.
- (32) Benabdoun, H. A.; Kulbay, M.; Rondon, E.-P.; Vallières, F.; Shi, Q.; Fernandes, J.; Fahmi, H.; Benderdour, M. In Vitro and in Vivo Assessment of the Proresolutive and Antiresorptive Actions of Resolvin D1: Relevance to Arthritis. *Arthritis Research & Therapy* **2019**, *21* (1), 72. <https://doi.org/10.1186/s13075-019-1852-8>.
- (33) Liu, Y.; Zhou, D.; Long, F.-W.; Chen, K.-L.; Yang, H.-W.; Lv, Z.-Y.; Zhou, B.; Peng, Z.-H.; Sun, X.-F.; Li, Y.; Zhou, Z.-G. Resolvin D1 Protects against Inflammation in Experimental Acute Pancreatitis and Associated Lung Injury. *American Journal of Physiology-Gastrointestinal and Liver Physiology* **2016**, *310* (5), G303–G309. <https://doi.org/10.1152/ajpgi.00355.2014>.

- (34) Grobe, J. L.; Mecca, A. P.; Lingis, M.; Shenoy, V.; Bolton, T. A.; Machado, J. M.; Speth, R. C.; Raizada, M. K.; Katovich, M. J. Prevention of Angiotensin II-Induced Cardiac Remodeling by Angiotensin-(1-7). *Am J Physiol Heart Circ Physiol* **2007**, *292* (2), H736-742. <https://doi.org/10.1152/ajpheart.00937.2006>.
- (35) Borlaug, B. A. Evaluation and Management of Heart Failure with Preserved Ejection Fraction. *Nature Reviews Cardiology* **2020**, *17* (9), 559–573. <https://doi.org/10.1038/s41569-020-0363-2>.
- (36) Halade, G. V.; Kain, V.; Serhan, C. N. Immune Responsive Resolvin D1 Programs Myocardial Infarction-Induced Cardiorenal Syndrome in Heart Failure. *FASEB J.* **2018**, *32* (7), 3717–3729. <https://doi.org/10.1096/fj.201701173RR>.
- (37) Saito, P.; Melo, C. P. B.; Martinez, R. M.; Fattori, V.; Cezar, T. L. C.; Pinto, I. C.; Bussmann, A. J. C.; Vignoli, J. A.; Georgetti, S. R.; Baracat, M. M.; Verri, W. A. J.; Casagrande, R. The Lipid Mediator Resolvin D1 Reduces the Skin Inflammation and Oxidative Stress Induced by UV Irradiation in Hairless Mice. *Front. Pharmacol.* **2018**, *9*. <https://doi.org/10.3389/fphar.2018.01242>.
- (38) Bürgin-Maunders, C. S.; Nataatmadja, M.; Vella, R. K.; Fenning, A. S.; Brooks, P. R.; Russell, F. D. Investigation of Long Chain Omega-3 PUFAs on Arterial Blood Pressure, Vascular Reactivity and Survival in Angiotensin II-Infused Apolipoprotein E-Knockout Mice. *Clin. Exp. Pharmacol. Physiol.* **2016**, *43* (2), 174–181. <https://doi.org/10.1111/1440-1681.12520>.
- (39) Shen, T.; Xing, G.; Zhu, J.; Zhang, S.; Cai, Y.; Li, D.; Xu, G.; Xing, E.; Rao, J.; Shi, R. Effects of 12-Week Supplementation of Marine Omega-3 PUFA-Based Formulation Omega3Q10 in Older Adults with Prehypertension and/or Elevated

Blood Cholesterol. *Lipids Health Dis* **2017**, *16* (1), 253.

<https://doi.org/10.1186/s12944-017-0617-0>.

(40) Haudek, S. B.; Cheng, J.; Du, J.; Wang, Y.; Hermosillo-Rodriguez, J.; Trial, J.; Taffet, G. E.; Entman, M. L. Monocytic Fibroblast Precursors Mediate Fibrosis in Angiotensin-II-Induced Cardiac Hypertrophy. *J Mol Cell Cardiol* **2010**, *49* (3), 499–507. <https://doi.org/10.1016/j.yjmcc.2010.05.005>.

(41) Sriramula, S.; Francis, J. Tumor Necrosis Factor - Alpha Is Essential for Angiotensin II-Induced Ventricular Remodeling: Role for Oxidative Stress. *PLoS One* **2015**, *10* (9). <https://doi.org/10.1371/journal.pone.0138372>.

(42) Senchenkova Elena Y.; Russell Janice; Yildirim Alper; Granger D. Neil; Gavins Felicity N.E. Novel Role of T Cells and IL-6 (Interleukin-6) in Angiotensin II-Induced Microvascular Dysfunction. *Hypertension* **2019**, *73* (4), 829–838. <https://doi.org/10.1161/HYPERTENSIONAHA.118.12286>.

(43) Lima, V. V.; Zemse, S. M.; Chiao, C.-W.; Bomfim, G. F.; Tostes, R. C.; Clinton Webb, R.; Giachini, F. R. Interleukin-10 Limits Increased Blood Pressure and Vascular RhoA/Rho-Kinase Signaling in Angiotensin II-Infused Mice. *Life Sci* **2016**, *145*, 137–143. <https://doi.org/10.1016/j.lfs.2015.12.009>.

Figure legends

Figure 1: RvD1 suppresses neutrophil and monocyte infiltration in cardiac tissue.

A) HE staining was performed to assess infiltration tissue formation in mice infused with Ang-II (1.5 mg/kg/day) for 7 or 14 days followed by dairy administration of RvD1 (3 µg/kg/day); the scale bar represents 200 µm. Leukocyte subpopulation infiltration at 7 or 14 days was determined by IHC against neutrophils (B) and monocytes (C), followed by densitometry of the stained area; the scale bar represents 100 µm. For all experiments, one-way ANOVA with Tuckey's test was used and exact p values are shown with their respective pairwise comparisons in the scatter plots. n=6 for all experimental groups.

Figure 2: RvD1 decreases cardiac VCAM-1 and ICAM-1 levels. Expression of cellular adhesion molecules is shown in (A) for ICAM-1 and VCAM-1 (B). Cardiac tissue of mice infused with Ang-II (1.5 mg/kg/day) for 7 or 14 days plus RvD1 treatment (3 µg/kg/day) was processed for IHC and measured by densitometry (C); the scale bar represents 100 µm. For all experiments, one-way ANOVA with Tuckey's test was used and exact p values are shown with their respective pairwise comparisons in the scatter plots. n=6 for all experimental groups.

Figure 3: RvD1 reduces circulating pro-inflammatory cytokines. Mice were infused with Ang-II (1.5 mg/kg/day) for 7 or 14 days followed by dairy administration of RvD1 (3 µg/kg/day) and blood was acquired for plasma extraction and further cytokine quantification by multiplex assay. For all experiments, one-way ANOVA with Tuckey's test was used and exact p values are shown with their respective pairwise comparisons in the scatter plots. n=6 for all experimental groups.

Figure 4: RvD1 partially prevents cardiac hypertrophy. A) HE staining of mice hearts infused with Ang-II (1.5 mg/kg/day) for 7 or 14 days and concomitant RvD1 (3 µg/kg/day) treatment; the scale bar represents 2 mm. B) Representative images of harvested hearts and measurement of the HW/TL ratio; the scale bar represents 5 mm. C) CM area was assessment through WGA staining; the scale bar represents 50 µm. For all experiments, one-way ANOVA with Tuckey's test was used and exact p values are shown with their respective pairwise comparisons in the scatter plots. n=6 for all experimental groups.

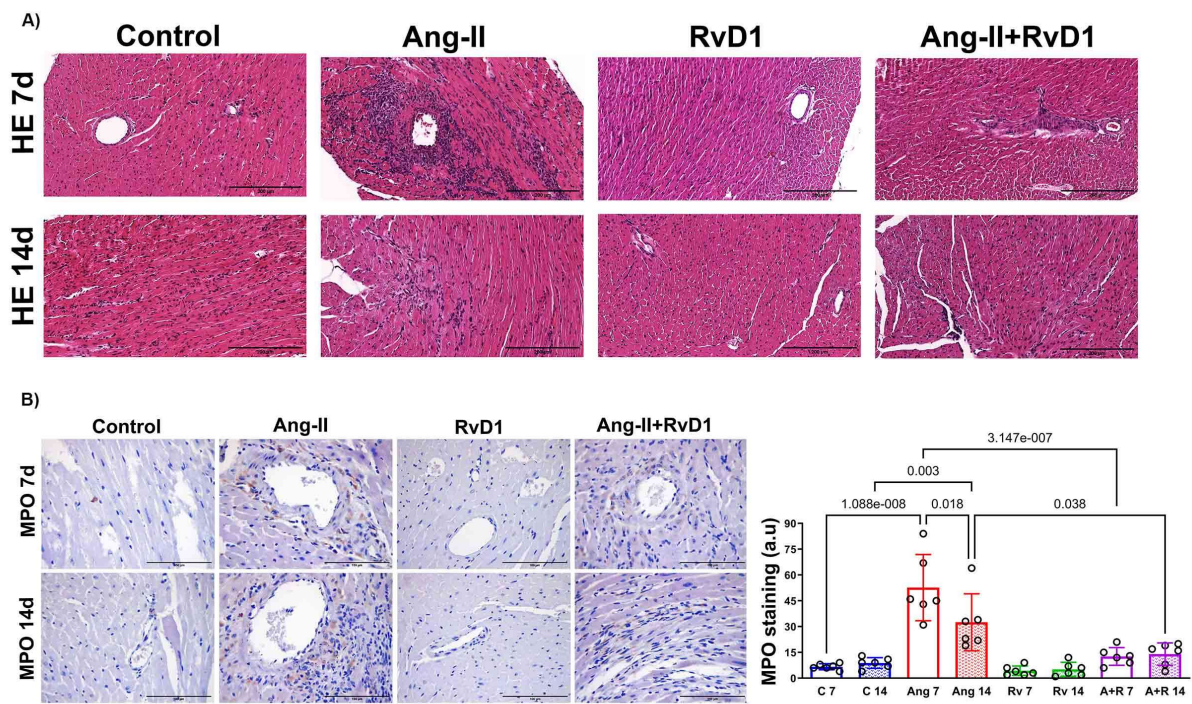
Figure 5: RvD1 restores cardiac functional parameters. A) Representative M-mode echocardiography images from mice infused with Ang-II (1.5 mg/kg/day) for 7 or 14 days, followed by daily RvD1 (3 µg/kg/day) administration; the scale bar is presented in cm. B) Analysis of cardiac functional parameters: interventricular septal wall thickness (IVWST), posterior wall thickness (PWT), left ventricular end-diastolic and end-systolic diameters (LVEDd and LVESd), ejection fraction (EF) and fractional shortening (FS). For all experiments, one-way ANOVA with Tuckey's test was used and exact p values are shown with their respective pairwise comparisons in the scatter plots. n=6 for all experimental groups.

Figure 6: RvD1 partially decreases cardiac collagen deposition. Ang-II (1.5 mg/kg/day) was delivered to mice together with daily RvD1 (3 µg/kg/day) administration, and cardiac fibrosis was elucidated by Masson's trichrome staining at 7 days (A) or 14 days (B) of infusion; the scale bar represents 200 µm. C) Collagen deposition area was measured by color deconvolution and densitometry at the interstitial (IS) and perivascular (PV). For all experiments, one-way ANOVA with Tuckey's test was used and exact p values are shown with their respective pairwise comparisons in the scatter plots. n=6 for all experimental groups.

Figure 7: RvD1 attenuates HBP development. Ang-II (1.5 mg/kg day) was delivered to mice for 7 or 14 days, with concomitant daily treatment of RvD1 (3 µg/kg/day). Systolic (SAP, A), diastolic (DAP, B), mean blood pressure (MAP, C) and heart frequency (BPM) were obtained through the tail-cuff method and further analyzed. For all experiments, one-way ANOVA with Tuckey's test was used and exact p values are shown with their respective pairwise comparisons in the scatter plots. n=6 for all experimental groups.

Figures

Figure 1 FALTAN LOS MONOCITOS



C)

IHC contra monocitos pendiente

Figure 2

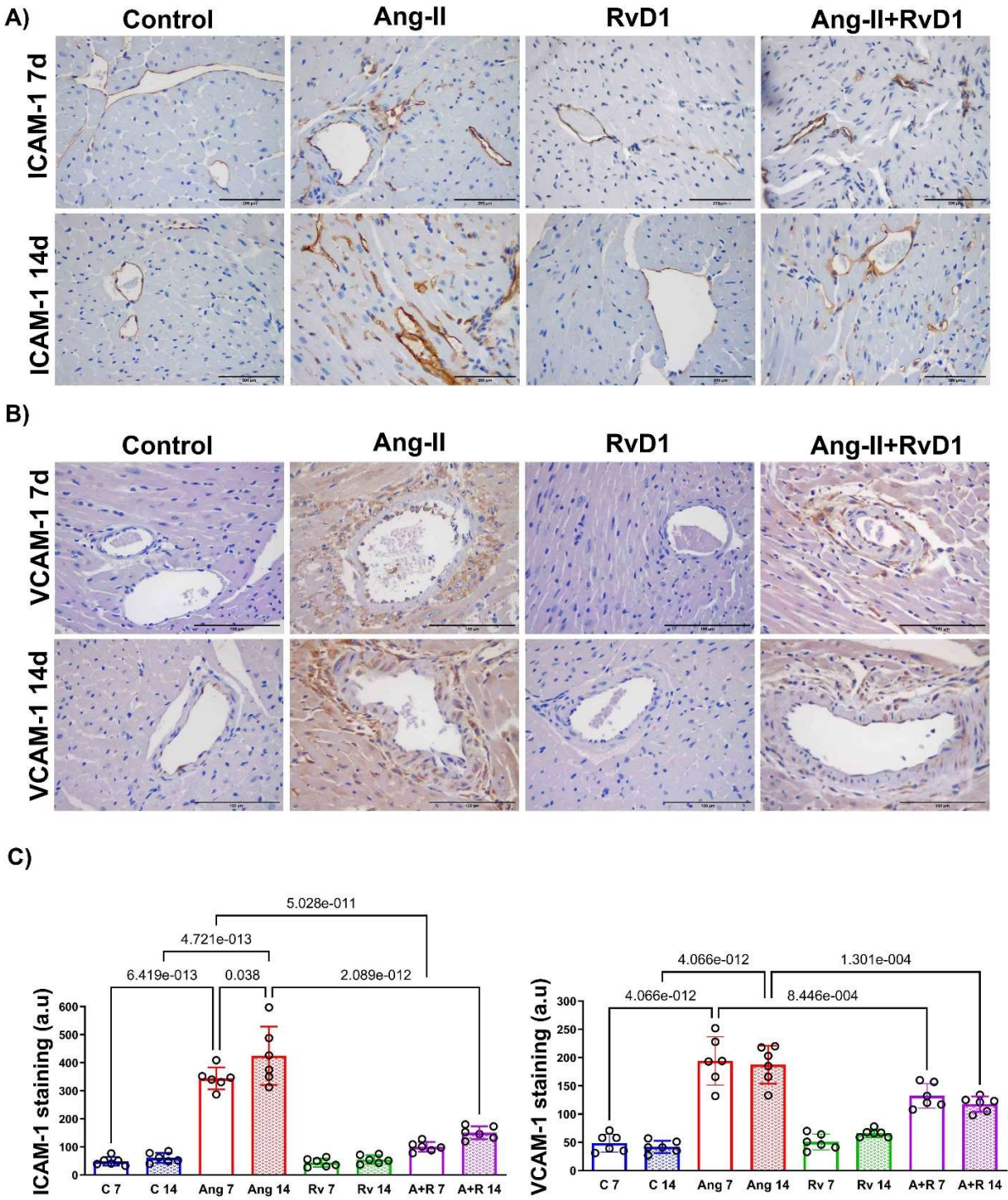


Figure 3

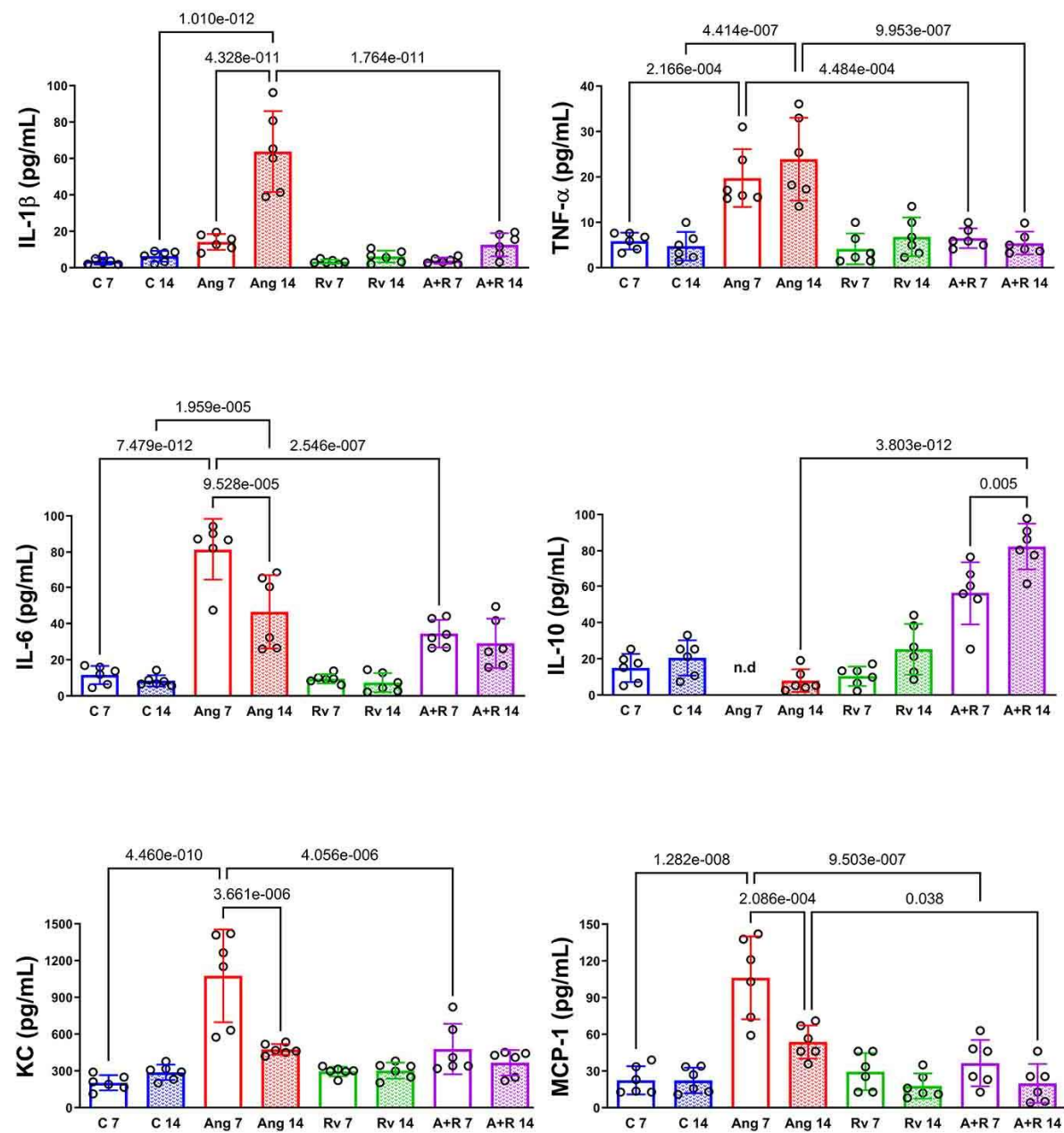


Figure 4

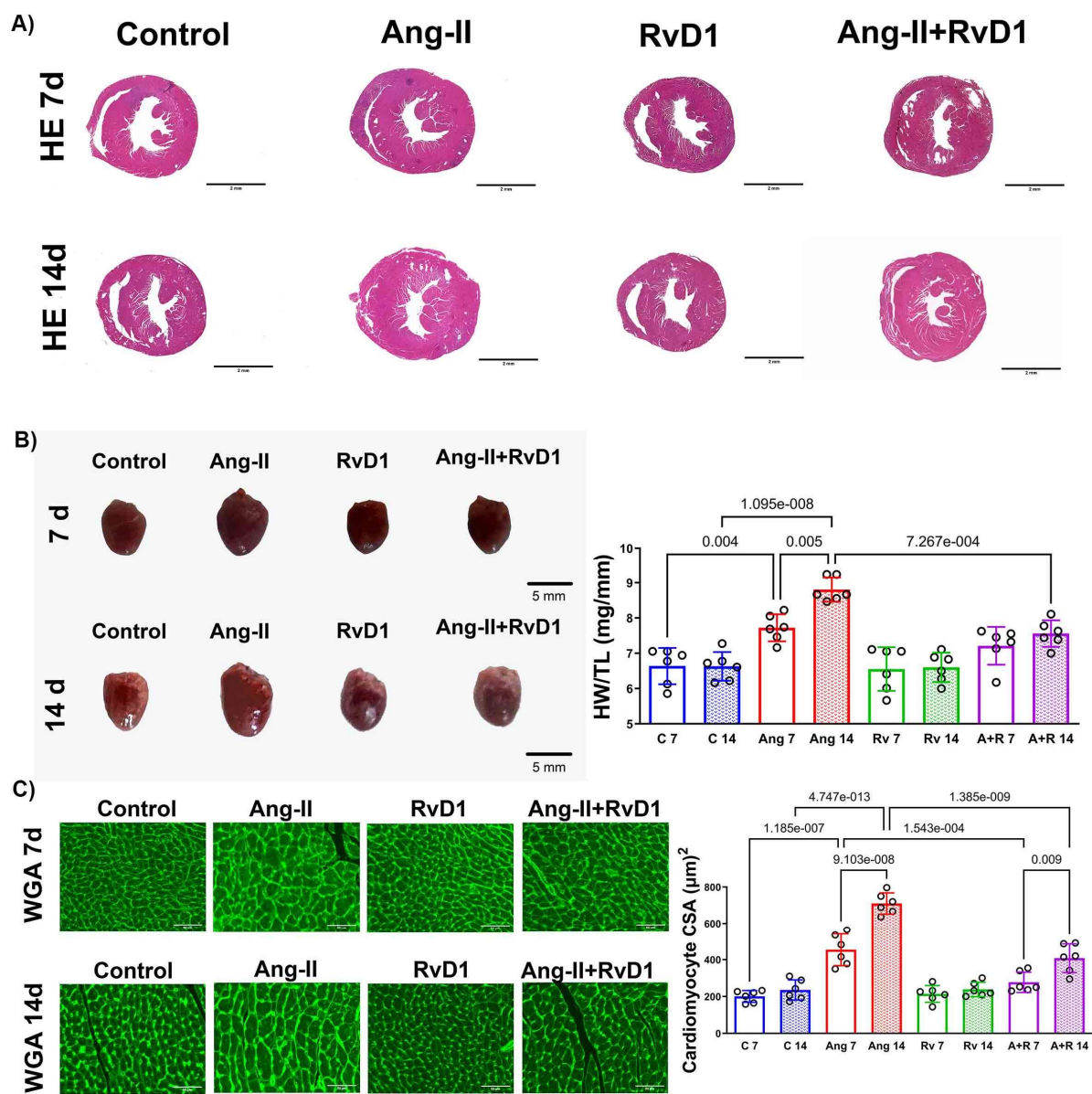


Figure 5

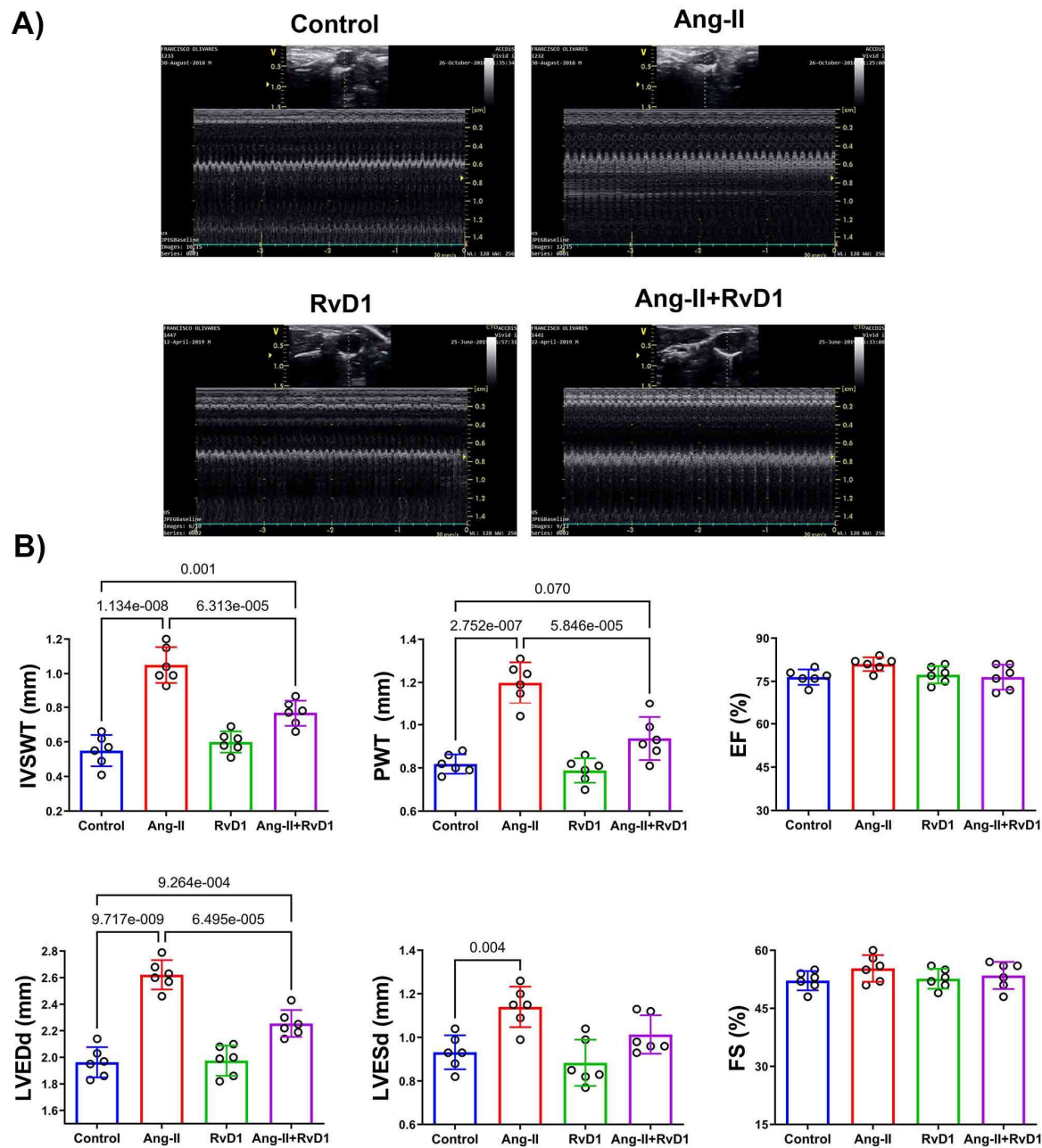


Figure 6

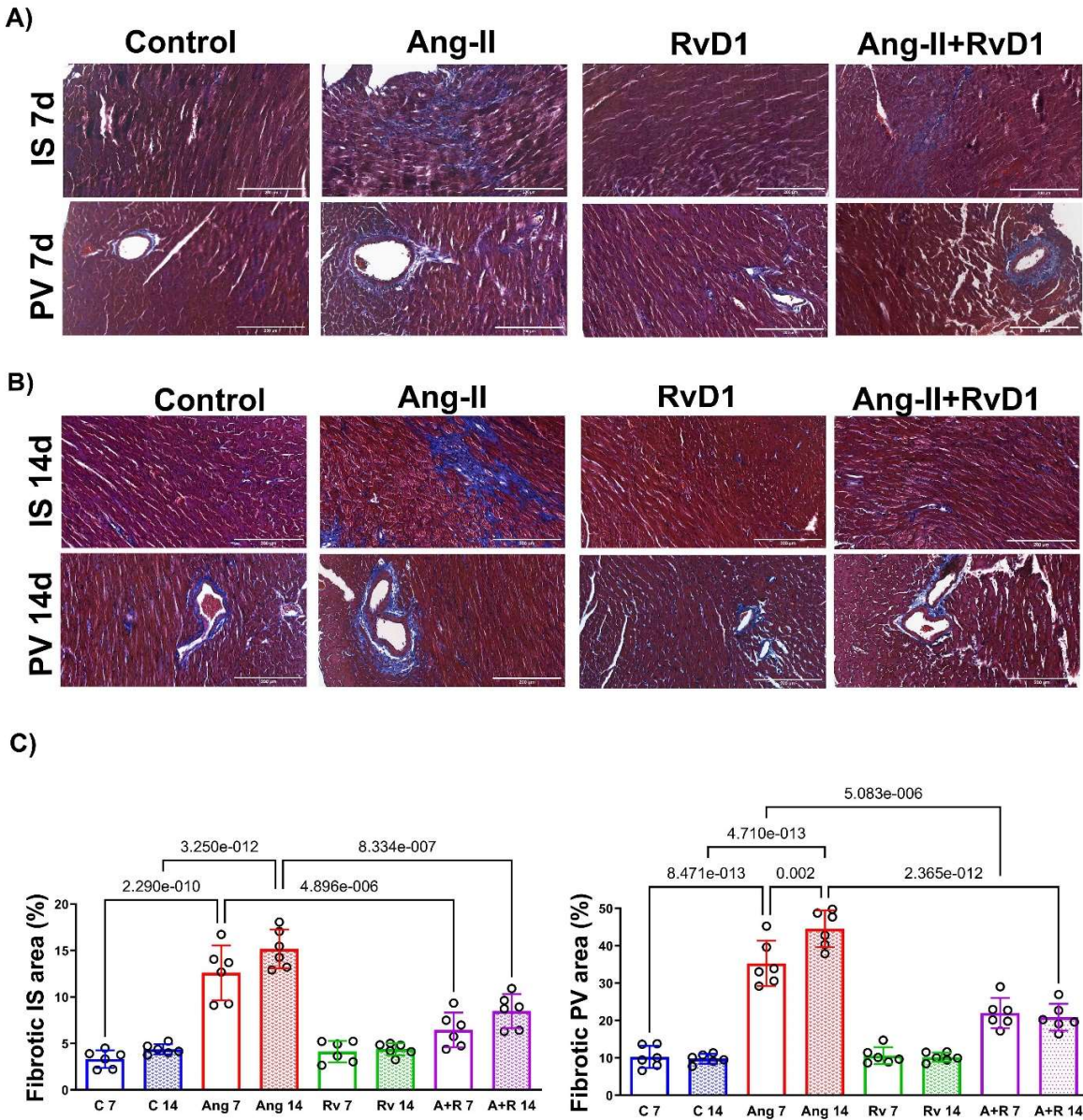


Figure 7

